This is a repository copy of *Isospin symmetry breaking in the T=1, A=70 triplet*.

White Rose Research Online URL for this paper:
https://eprints.whiterose.ac.uk/id/eprint/216585/

Version: Published Version

Isospin symmetry breaking in the $T = 1$, $A = 70$ triplet

G. L. Zimba [1,*] P. Ruotsalainen,[1] G. De Gregorio,[2,3] G. de Angelis,[4] J. Sarén,[1] J. Uusitalo,[1] K. Auranen,[1]
A. D. Briscoe,[1,†] Z. Ge,[1] T. Grahn,[1] P. T. Greenlees,[1] A. Illana,[1,‡] D. G. Jenkins,[5] H. Joukainen,[1] R. Julin,[1]
H. Jutila,[1] A. Kankainen,[1] J. Louko,[1] M. Luoma,[1] J. Ojala,[1] J. Pakarinen,[1] A. Raggio,[1] P. Rahkila,[1] J. Romero,[1,6]
M. Stryjczyk,[1] A. Tolosa-Delgado,[1,§] R. Wadsworth,[5] and A. Zadvornaya[1,‖]

[1]*Accelerator Laboratory, Department of Physics, University of Jyväskylä, FI-40014 Jyväskylä, Finland*
[2]*Dipartmento di Matematica e Fisca, Università degli Studi della Campania "Luigi Vanvitelli," I-81100 Caserta, Italy*
[3]*Istituto Nazionale di Fisica Nucleare, Sezione di Napoli, IT-80126 Napoli, Italy*
[4]*Istituto Nazionale di Fisica Nucleare, Laboratori Nazionali di Legnaro, I-35020 Legnaro, Italy*
[5]*School of Physics, Engineering and Technology, University of York, Heslington, York Y010 5DD, United Kingdom*
[6]*Department of Physics, Oliver Lodge Laboratory, University of Liverpool, Liverpool L69 7ZE, United Kingdom*

Excited states in the ^{70}Kr and ^{70}Br nuclei were populated via the ^{40}Ca(^{32}S, $2n$) ^{70}Kr and ^{40}Ca(^{32}S, pn) ^{70}Br fusion-evaporation reactions at the Accelerator Laboratory of the University of Jyväskylä. The $2^+ \longrightarrow 0^+$ and $4^+ \longrightarrow 2^+$ transitions in ^{70}Kr have been found to be 881(1) keV and (tentatively) 1037(2) keV, respectively. Several new γ-ray transitions were also identified in ^{70}Br, and the $T = 1$ band has been tentatively extended up to $J^\pi = 10^+$. The newly observed transitions in ^{70}Kr and ^{70}Br resolve discrepancies in the previously reported results for these nuclei. The experimental Coulomb, triplet, and mirror energy differences are compared with the results of two independent shell-model calculations. The comparisons aim to investigate the shape evolution and the role of the isospin breaking interactions in this mass region.

I. INTRODUCTION

In the framework of isospin symmetry, the interactions between proton-proton (pp), neutron-neutron (nn), and proton-neutron (pn) pairs are regarded identical. Neutrons and protons are distinguishable via their isospin projection quantum numbers $t_z = \pm 1/2$, respectively. In a multinucleon system, the total isospin projection, denoted as T_z, is determined by the sum of the isospin quantum numbers of the individual nucleons, given by $T_z = (N - Z)/2$, where N and Z are the neutron and proton numbers, respectively. Therefore, an isobaric triplet consists of the $T_z = -1$, 0, and $+1$ nuclei such as ^{70}Kr ($N = Z - 2$), ^{70}Br ($N = Z$), and ^{70}Se ($N = Z + 2$) as discussed in the present work. A given nucleus can have excited states labeled with the total isospin quantum number T ranging from $|N - Z|/2$ to $|N + Z|/2$. In the $T_z = -1$ and

$+1$ systems, the lowest-lying states are $T = 1$, but in the $T_z = 0$ member of the triplet, both $T = 0$ and $T = 1$ states are expected. The states with the same T ($T = 1$ for the current case) within an isobaric triplet are termed as isobaric analog states (IAS). Moreover, the IAS are expected to be degenerate in terms of the excitation energy in the absence of any electromagnetic forces and if the isospin symmetry is preserved. However, experiments show differences in the energies of IAS, which can be mainly attributed to Coulomb repulsion between protons, but also other effects have been identified, as will be discussed below [1].

The energy differences between IAS in the odd-odd $N = Z$ and even-even $N = Z + 2$ nuclei, called the Coulomb energy differences, CED $= E_x(J^\pi, T_z = 0) - E_x(J^\pi, T_z = +1)$, where E_x is the excitation energy of a state with spin-parity J^π. CED have shown to be a sensitive probe for investigating both the microscopic and macroscopic nuclear structure. CED have been employed to gain insights into various aspects, such as the alignment of valence nucleons [2], shape changes as a function of spin [3], and the evolution of nuclear radii along the yrast line [4]. In addition, the mirror energy differences (MED), defined as MED $= E_x(J^\pi, T_z = -1) - E_x(J^\pi, T_z = +1)$ and the triplet energy differences (TED), defined as TED $= E_x(J^\pi, T_z = -1) + E_x(J^\pi, T_z = +1) - 2E_x(J^\pi, T_z = 0)$ have been used to investigate the isovector and isotensor components of the nuclear interaction, respectively [1,5]. During the past few decades a wealth of evidence has been collected for an additional isospin nonconserving (INC) interaction, which is

---

*Contact author: zimba@frib.msu.edu; Present address: Facility for Rare Isotope Beams, Michigan State University, 640 South Shaw Lane, East Lansing, Michigan 48824, USA.

†Present address: Department of Physics, Oliver Lodge Laboratory, University of Liverpool, P. O. Box 147, Liverpool L69 7ZE, United Kingdom.

‡Present address: Grupo de Física Nuclear, EMFTEL and IPAR-COS, Universidad Complutense de Madrid, 28040 Madrid, Spain.

§Present address: European Organization for Nuclear Research (CERN), Geneva, Switzerland.

‖Present address: University of Edinburgh, Edinburgh, EH9 3FD, United Kingdom.

required in the theoretical calculations to explain the observed experimental CED, MED, and TED data [1,6–10].

The region around the $N = Z$, $A = 70$ nuclei is known to exhibit rapid structural evolution, especially in terms of the nuclear shapes. The shape evolution and the occurrence of shape coexistence, supported for example by the experimental observation of shape isomers [11,12], makes this region particularly interesting to study. The neutron-deficient Se and Kr isotopes have been found to evolve from prolate ground-state shapes towards oblate shapes as the $N = Z$ line is approached and crossed (see, e.g., Ref. [13] and references therein). The reason for the rapid shape changes in this region is understood to result from the deformed shell gaps at the nucleon numbers 34 and 36 (oblate), and 34 and 38 (prolate) [11]. Interestingly, the CED trend for the mass $A = 70$ pair (^{70}Br and ^{70}Se) has been found to be negative, unlike for the other known cases in the region [3,14]. The reason for this unique behavior has been attributed to the shape-evolution effects [3,15]. It has also been suggested that the $g_{9/2}$ intruder orbital and its interplay with the fp-shell orbitals plays a vital role in determining the overall properties of the nuclei in this region [6,7].

An interesting finding for the $B(E2; 0^+ \longrightarrow 2^+)$ values within the $A = 70$ triplet was recently published in Ref. [16]. The proton matrix elements, derived from the $B(E2)$ values, should follow a linear relationship as a function of T_z, assuming that the isospin symmetry is not significantly broken and the nuclear shapes within the triplet remain similar. However, Ref. [16] suggested a significant shape change between ^{70}Kr and ^{70}Se owing to the large measured $B(E2)$ value for ^{70}Kr. This interpretation was later questioned in Ref. [17], where it was pointed out that the reason for the observed nonlinearity could be due to ^{70}Br, rather than ^{70}Kr. Here, the main argument was a potential unobserved decay branch from the 2^+ state to a low-lying 1^+ state in ^{70}Br, which would cause the measured $B(E2; 0^+ \longrightarrow 2^+)$ value for ^{70}Br to be underestimated if not corrected for the potential branching. In the lighter odd-odd $N = Z$ nuclei ^{62}Ga and ^{66}As the 1^+ states are known to be located below the $T = 1$, 2^+ states [9,18]. The recent ^{70}Kr β-decay study reported in Ref. [19] observed a new 1^+ state in ^{70}Br at 1120 keV, which was concluded to be the lowest one. If there would be another low-lying 1^+ state (below 511 keV) in ^{70}Br, the experiment of Ref. [19] could not potentially observe this due to the high Compton background created by the 511-keV annihilation γ rays. This debate motivates the investigation of the level structure in ^{70}Br at the low excitation energy.

Two independent fusion-evaporation reaction experiments were conducted to investigate the excited states in ^{70}Br [14,20]. These experiments suggested consistent excitation energies for the 2^+ and 4^+ states in the $T = 1$ band. However, regarding the $T = 1$, 6^+ state, there is a disagreement between these two experiments, in addition to some other minor differences. Neither of these studies observed excited states below the $T = 1$, 2^+ state.

Candidates for the excited states in ^{70}Kr were reported for the first time in Ref. [8], yielding values of 870 and 1867 keV for the 2^+ and 4^+ states, respectively. In a more recent study by Wimmer *et al.* [13], the 2^+ and 4^+ states were measured to be located at 884 and 1913 keV, respectively. The

extracted MED and TED values highlight the disagreement between these two experiments. The values for the TED and MED for the 2^+ and 4^+ states change by $+14$ and $+46$ keV, respectively, when replacing the excitation energies from Ref. [8] with those from Ref. [13]. This change is noteworthy because it results in better agreement between the experiment and the theoretical TED predictions, which do not incorporate the additional INC interaction [7]. It was also found that there is no need to include an INC term to reproduce the TED for the $J^\pi = 4^+$ state in the $A = 62$ triplet [21].

This article reports new experimental data for ^{70}Kr and ^{70}Br obtained using the selective recoil-β and recoil-β-β correlation methods, which make use of the short ground-state β-decay half-lives and high β-decay endpoint energies of ^{70}Kr and ^{70}Br [22–24]. These data are used to resolve the conflicts between Refs. [14,20] for ^{70}Br and Refs. [8,13] for ^{70}Kr as discussed above. Precisely determining the excitation energies of the $T = 1$ states in the $N = Z - 2$, ^{70}Kr and $N = Z$, ^{70}Br nuclei is essential for investigating the role of the isospin breaking effects in this mass region. The new experimental results are compared with the shell-model predictions for the CED, MED, and TED values within the $A = 70$ isobaric triplet.

II. EXPERIMENTAL DETAILS

The ^{70}Kr and ^{70}Br nuclei were produced at the Accelerator Laboratory of the University of Jyväskylä (JYFL-ACCLAB), using the ^{40}Ca(^{32}S, $2n$) and ^{40}Ca(^{32}S, pn) fusion-evaporation reactions, respectively. In this experiment, the ^{32}S beam with an average intensity of 5 pnA was accelerated by the K130 cyclotron to an energy of 92 MeV and bombarded a 0.6-mg/cm^2-thick ^{nat}Ca target for 280 h. Prompt γ rays were detected at the target position using the JUROGAM 3 germanium-detector array [25]. The Jyväskylä-York University Tube (JYUTube) scintillator detector array surrounded the target position to veto or select reaction channels based on the number of detected charged particles that evaporate in the reaction. The fusion recoils were further separated from the unreacted beam and other reaction products using the vacuum-mode mass-separator, Mass Analyzing Recoil Apparatus (MARA) [26], which was set to transmit mass $A = 70$ recoils to its focal plane. Furthermore, the MARA mass-slit system was employed to prevent other masses arriving to the focal plane. It is important to note that MARA separates recoils based on their kinetic energy and mass-to-charge ratio (A/Q). However, due to the finite A/Q resolution, some fraction of the neighboring masses are transmitted to the separator focal plane. In particular, the reaction products having similar A/Q ratio as the reference particle go through MARA. For this reason, ^{66}As, which is a fast β emitter [27] produced in the αpn channel, was also transmitted to the focal plane.

The MARA focal plane setup consisted of a multiwire proportional counter (MWPC) to measure the recoil position and time-of-flight, together with a 700-μm thick double-sided silicon strip detector (DSSSD) with 192×72 strips located 30 cm downstream from the MWPC. The DSSSD detector was also used to detect the recoil implantation and its subsequent β decay allowing for recoil-decay correlations. Since
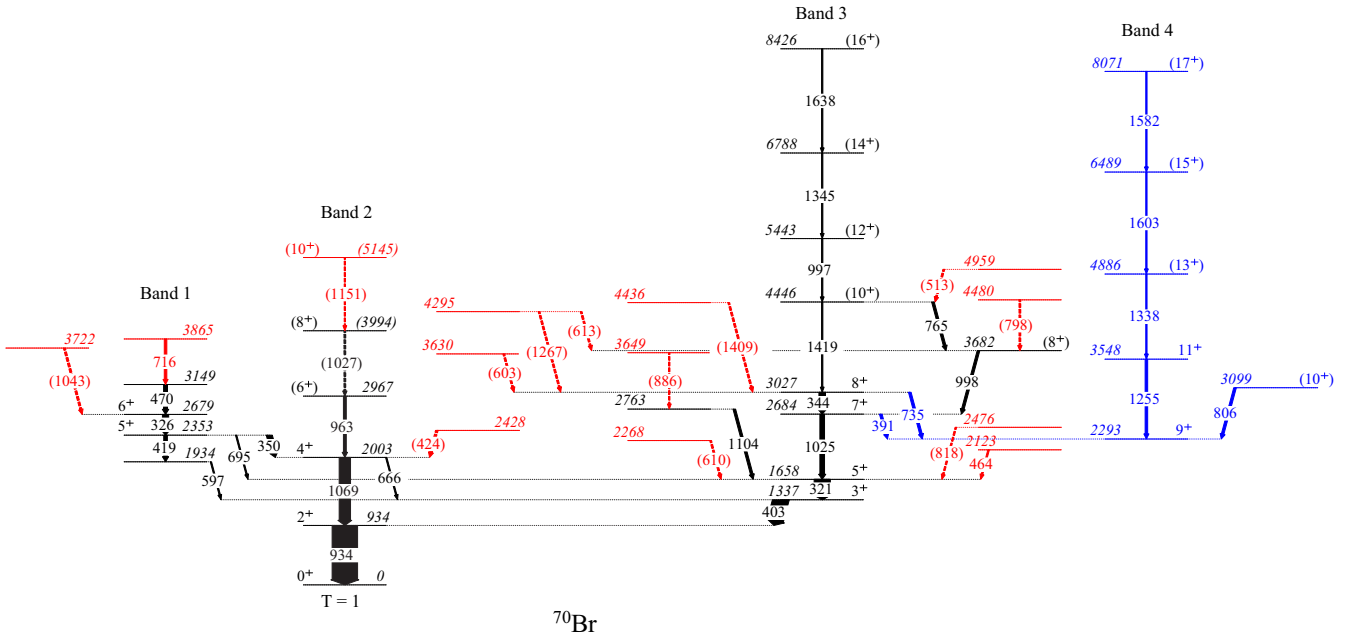
FIG. 1. Level scheme of ^{70}Br deduced in the present work. The width of the arrows are proportional to the intensity of the γ-ray transitions. The intensities of the γ-ray transitions are extracted from the recoil-β-tagged γ-singles or γ-γ coincidence data. Newly assigned levels and γ-ray transitions are labeled in red. Previously observed transitions in Refs. [14,20], which were also observed in the present work, are labeled in black. The transitions labeled in blue have been observed in the current work; however, the order of these transitions has been obtained from Ref. [20].

the β particles pass through the DSSSD providing only a ΔE signal, the plastic scintillator detector Tuike [28] was installed after the DSSSD to detect and measure the full remaining energy of the β particles.

The ^{70}Kr and ^{70}Br reaction products were identified at the MARA focal plane based on their characteristic β-decay properties. The relatively short β-decay half-lives and high β-decay end point energies of ^{70}Kr ($t_{1/2} = 45.19(14)$ ms [19], $Q_{EC} = 10330(200)$ keV [22]) and ^{70}Br ($t_{1/2} = 78.42(51)$ ms [23], $Q_{EC} = 10504(15)$ keV [24]), allowed the application of the recoil-β and recoil-β-β tagging methods [29,30] to identify the prompt γ rays originating from these nuclei.

III. RESULTS FOR THE $N = Z$ NUCLEUS ^{70}Br

The level scheme of ^{70}Br deduced in the present work is shown in Fig. 1. Details of the observed γ-ray transitions are listed in Table I. These results are based on the recoil-β tagged γ-ray singles and $\gamma - \gamma$ coincidence analysis with the condition that at most one charged particle is detected in the JYUTube scintillator detector. The lower limits of the β-particle energy gates were varied between 3 and 5 MeV for different γ-ray gates to reduce the contribution from the contaminant channels.

A. Band 1

Figure 2(a) shows the gated γ-ray spectrum with the gate set on the 350-keV γ ray in ^{70}Br. Strong coincidences with 326-, 470-, 716-, 934-, and 1069-keV transitions can be observed. The 934- and 1069-keV transitions were assigned in Refs. [14,20] to de-excite the the $T = 1$, 2^+, and 4^+ states,

respectively. In both of these works the 350-keV transition from a state at 2353 keV, was assigned to feed the $T = 1$, 4^+ state at 2003 keV and the 326-keV transition was placed to
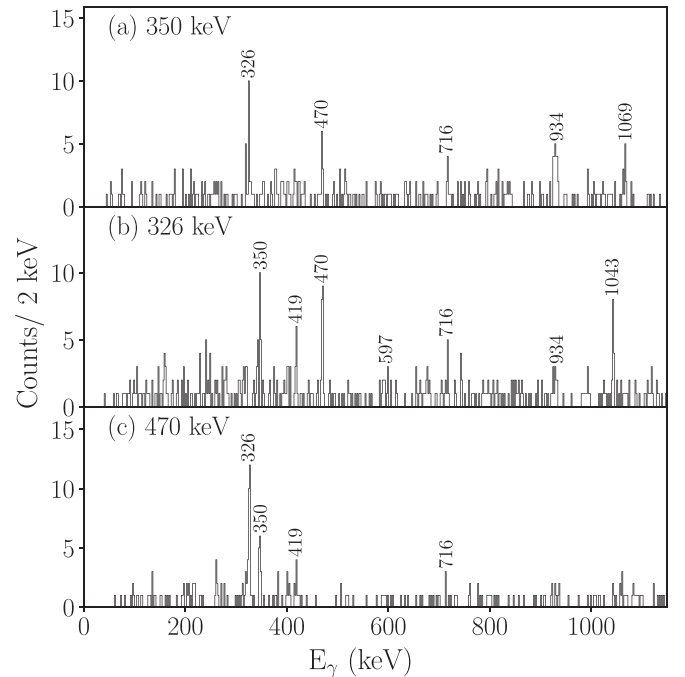

FIG. 2. Recoil-β tagged and gated $\gamma - \gamma$ coincidence spectra requiring detection of one charged-particle in JYUTube and using a correlation search time of 240 ms. The γ-ray gates have been set on (a) 350-keV, (b) 326-keV, and (c) 470-keV γ-ray transitions with a β-energy gate of 4–10 MeV.

TABLE I. The prompt γ-ray transitions measured for odd-odd ^{70}Br. The energy of the γ ray (E_γ), I_{re} relative γ-ray intensity normalized to the $2^+ \longrightarrow 0^+$ transition, energy of the initial level (E_i), energy of the final level (E_f), assigned spin and parity of the initial and final levels (I_i^π and I_f^π) are listed. The uncertainty on the energies of most transitions is around ± 1 keV, except for the weakest ones where an uncertainty of ± 2 keV is adopted. The transition and level energies for states connected to the 9^+ isomer, marked with an asterisk (*), have been adopted from Ref. [20]. The intensities of the γ-ray transitions associated with the isomer are not listed as it was not possible to normalize them.

E_γ (keV)	I_{re} (%)	E_i (keV)	E_f (keV)	I_i^π	I_f^π
321.1(10)	63(8)	1658.5(24)	1337.4(23)	5^+	3^+
325.9(11)	24(5)	2679.4(26)	2353.5(24)	6^+	5^+
343.8(10)	26(5)	3027.4(33)	2683.7(31)	8^+	7^+
350.3(11)	23(5)	2353.5(24)	2003.1(23)	5^+	4^+
391*	—	2683.7(31)	2293	7^+	9^+
403.4(14)	63(8)	1337.4(23)	934.1(19)	3^+	2^+
418.9(11)	14(4)	2353.5(24)	1934.6(24)	5^+	
424.3(10)	<10	2427.4(25)	2003.1(23)		4^+
464.1(11)	<10	2122.6(26)	1658.5(24)		5^+
469.9(11)	15(4)	3149.3(28)	2679.4(26)		6^+
512.9(11)	<10	4959.0(4)	4446.0(35)		(10^+)
597.2(10)	<10	1934.6(24)	1337.4(23)		3^+
602.6(11)	<10	3630.0(34)	3027.4(33)		8^+
609.9(11)	<10	2268.4(26)	1658.5(24)		5^+
612.8(11)	<10	4294.0(35)	3682.0(34)		(8^+)
665.8(11)	<10	2003.1(23)	1337.4(23)	4^+	3^+
694.9(11)	<10	2353.5(24)	1658.5(24)	5^+	5^+
716.0(10)	<10	3865.3(30)	3149.3(28)		
735*	—	3027.4(33)	2293	8^+	9^+
765.0(10)	17(4)	4446.0(35)	3682.0(34)	(10^+)	(8^+)
797.9(11)	<10	4479.6(40)	3682.0(34)		(8^+)
806*	—	3099	2293	(10^+)	9^+
818.0(10)	<10	2476.4(26)	1658.5(24)		5^+
886.0(18)	13(2)	3649.0(40)	2762.9(31)		
934.1(19)	100(10)	934.1(19)	0.0	2^+	0^+
963.4(17)	11(3)	2966.6(29)	2003.1(23)	(6^+)	4^+
996.7(20)	<10	5443.7(4)	4446.0(35)	(12^+)	(10^+)
998.0(20)	19(4)	3682.0(34)	2683.7(31)	(8^+)	7^+
1025.2(20)	18(4)	2683.7(31)	1658.5(24)	7^+	5^+
1027.1(20)	12(3)	3993.7(35)	2966.6(29)	(8^+)	(6^+)
1043.1(20)	<10.0	3722.5(33)	2679.4(26)		6^+
1068.8(20)	45(7)	2003.1(23)	934.1(19)	4^+	2^+
1104.4(20)	15(4)	2762.9(31)	1658.5(24)		5^+
1151.3(20)	<10	5145.0(4)	3993.7(35)	(10^+)	(8^+)
1255*	—	3548	2293	11^+	9^+
1267.1(20)	<10	4294.0(35)	3027.4(33)		8^+
1338*	—	4886	3548	(13^+)	11^+
1345.3(20)	<10	6788.5(5)	5443.7(4)	(14^+)	(12^+)
1409.0(20)	<10	4436.0(40)	3027.4(33)		8^+
1418.6(20)	<10	4446.0(35)	3027.4(33)	(10^+)	8^+
1582*	—	8071	6489	(17^+)	(15^+)
1603*	—	6489	4886	(15^+)	(13^+)
1637.8(20)	<10	8426.5(5)	6788.5(5)	(16^+)	(14^+)

feed the 2353-keV state from a 2679-keV state. In the present data, the 470-keV transition is also seen in coincidence with the 350-keV transition and is therefore placed to feed the state at 2679 keV in agreement with Ref. [14]. The spin-parity assignments for the 2679-keV 6^+ and 2353-keV 5^+ states have been adopted from Ref. [20].

The γ-ray spectrum obtained by gating on the 326-keV γ ray, shown in Fig. 2(b), shows the 470- and 716-keV γ-ray transitions, which were also observed with the 350-keV gate. In addition, two relatively strong γ-ray peaks at 419 and 1043 keV are also observed in coincidence with the 326-keV γ ray. The 1043-keV γ ray is a new and is tentatively placed to feed the $T = 0$, 6^+ state at 2679 keV, while the 419-keV transition has been previously observed only in Ref. [14], but the energy was reported to be 421 keV instead. The observation of the 350- and 470-keV γ-ray transitions in Fig. 2(b)
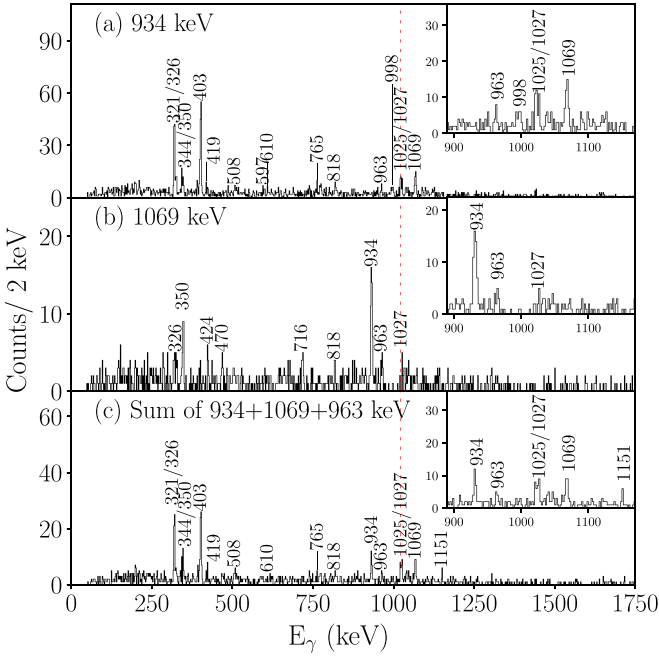
FIG. 3. Recoil-β tagged and gated $\gamma - \gamma$ coincidence spectra requiring detection of at most one charged-particle in JYUTube and using a correlation search time of 240 ms. The γ-ray gates have been set on (a) 934-keV and (b) 1069-keV transitions with a β-energy gate of 3–10 MeV. Panel (c) is showing the sum of gates on the 934-, 1069-, and 963-keV transitions with a β-energy gate of 5–10 MeV. The red dashed line represents the position of the previously known 1025-keV γ-ray transition.

provides support for their placement as depicted in Fig. 1. A transition with an energy of 597 keV was previously observed only in Ref. [14], and its assignment has been confirmed in the present work (see further discussion in Sec. III C). The 666- and 695-keV γ rays, which were assigned in the both previous works of Refs. [14,20], are not observed in Fig. 2 likely due to low statistics, but are clearly observed with the gates set on the strong 403- and 321-keV transitions discussed in Sec. III C.

In Fig. 2(c), the γ-ray gate is set on the 470-keV γ-ray transition. Figures 2(b) and 2(c) both show coincidences with the 419-keV γ-ray transition. Therefore, the 419-keV transition is assigned to de-excite the 5^+, 2353-keV state, consistent with the assignment made in Ref. [14]. Additionally, a new 716-keV γ-ray transition is observed with all 350-, 326-, and 470-keV gates. Hence, it is placed to feed the state at 3149 keV from a new state located at 3865 keV.

B. Band 2

Figure 3(a) shows the coincidence γ-ray spectrum obtained by gating on the $2^+ \longrightarrow 0^+$, 934-keV γ-ray transition in ^{70}Br. Several γ-ray lines are observed, notably those from the 963- and 1069-keV transitions. The 963-keV line is a candidate for the $T = 1$, $6^+ \longrightarrow 4^+$ transition in ^{70}Br. This assignment was also previously made in Ref. [14], but not in Ref. [20]. Furthermore, the 321- and 403-keV γ-ray transitions from the $T = 0$ band (Band 3) are also shown in Fig. 3(a). These transitions belong to the same cascade with

the relatively strong 1025- and 344-keV transitions. Closer inspection of the peak at 1025 keV shows a doublet-like structure with a second component at 1027 keV. In Ref. [14], a 1025-keV transition was placed on top of the 963-keV transition making it a candidate for the $T = 1$, $8^+ \longrightarrow 6^+$ transition in ^{70}Br. Such assignment was not made in Ref. [20].

Figure 3(b) shows the gate set on the 1069-keV γ rays. The resulting spectrum shows the strong coincidence with the 934-keV transition, but also peaks at 963 and 1027 keV are observed. The 1027-keV transition must be a doublet since the strong 1069- and 1025-keV transitions are located partially parallel. Therefore, the observed 1027-keV γ-ray transition is a plausible candidate for the $T = 1$, $8^+ \longrightarrow 6^+$ transition in ^{70}Br. The 1069-keV gate shows the structures in Band 1—the 350-keV transition, which is feeding the 4^+ state, in addition to the 326-, 470-, and 716-keV transitions, which are discussed in Sec. III A. Lastly, a coincidence is observed with a 424-keV line so this transition is tentatively placed to feed the 4^+ state from a new state at 2427 keV.

Figure 3(c) shows the coincidences with the sum of gates on the 934-, 1069-, and 963-keV γ-ray transitions. The doublet structure of the 1025-keV/1027-keV transitions become now more prominent with the majority of the intensity centered at 1027 keV. The sum of gates yields also a clear line at 1151 keV. These γ-rays could originate from the $10^+ \longrightarrow 8^+$ transition in the $T = 1$ band in ^{70}Br. Despite the limited statistics, which preclude an accurate angular distribution analysis and, therefore, firm spin assignments, it could be that the 963-, 1027-, and 1151-keV γ-ray transitions represent a cascade of stretched $E2$ transitions depopulating the excited 6^+, 8^+, and 10^+ states within the $T = 1$ band, respectively. This assumption is supported by the comparison with the isobaric analog states in ^{70}Se. The analog $T = 1$ band in ^{70}Se consists of the 945-, 1094-, 964-, 1034-, and 1168-keV γ-ray transitions [31,32].

Furthermore, Fig. 3 shows coincidences with γ rays at energies of 508, 818, and 610 keV. It appears that these transitions are new in ^{70}Br. The 818-keV transition is seen in a strong coincidence with the 934-keV transition, but it appears also in the spectrum gated by the 1069-keV line, but significantly weaker. The 818-keV line is also seen in coincidence with the transitions in Band 3 (especially with the 321- and 403-keV transitions), so this transition is tentatively placed to feed the 5^+ state at 1658 keV. The 508-keV transition could not be placed in the current analysis, but it is likely that this γ ray belongs to ^{70}Br. The 610-keV line is also seen in coincidence with the 321- and 403-keV transitions, so it is assigned to feed the 1658-keV 5^+ state.

C. Band 3

Figure 4(a) shows the γ rays in coincidence with the strong 403-keV γ-ray transition. In the previous works this transition was placed to feed the 2^+ state from a 3^+ state at 1337 keV, which in turn is fed by a strong 321-keV transition from a 5^+, 1658-keV state. The strongest coincidences with the 403-keV gate are seen with the 321-, 934-, 344-, and 1025-keV transitions. The coincidences with the 403- and 321-keV transitions are now particularly interesting, since
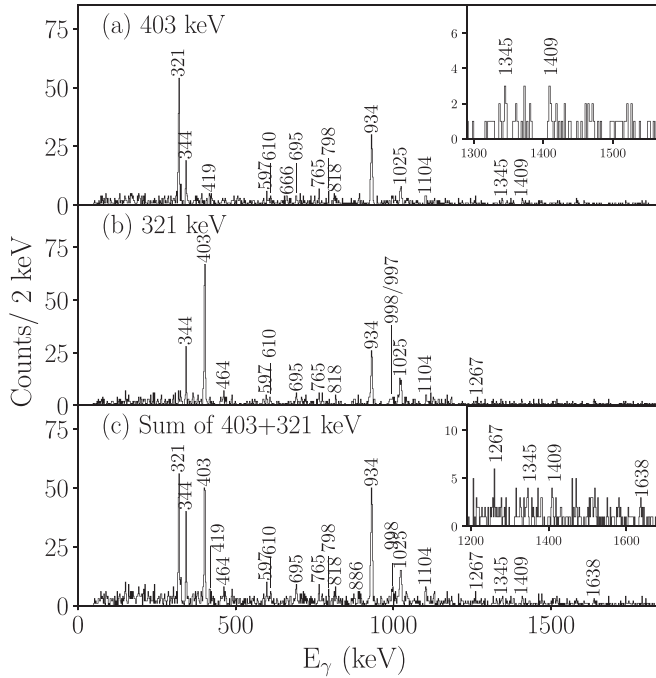
FIG. 4. Recoil-β tagged and gated $\gamma - \gamma$ coincidence spectra with at most one charged-particle detected in JYUTube and using a correlation search time of 240 ms. The γ-ray gates have been set on (a) 403-keV and (b) 321-keV transitions using β-energy gates of 4–10 MeV and 3–10 MeV, respectively. Panel (c) is showing the sum of gates on the 403- and 321-keV transitions with a β-energy gate of 4–10 MeV.

FIG. 5. Recoil-β tagged and gated $\gamma - \gamma$ coincidence spectra requiring detection of at most one charged-particle in JYUTube and using a correlation search time of 240 ms. The γ-ray gates have been set on (a) 1025-keV, (b) 344-keV, and (c) is showing the sum of gates on the 998-, 765-, and 1418-keV transitions with a β-energy gate of 4–10 MeV. The origin of the peak labeled in gray could not be confirmed in the present analysis.

potential links to an unobserved 1^+ state can be explored, and if such a state is located below the 934-keV 2^+ state.

The observed 321-, 1025-, and 344-keV transitions form a cascade up to an 8^+ state at 3027 keV, as deduced in the both previous works [14,20]. In Ref. [20] this cascade was suggested to continue with the 1419-, 997-, 1345-, and 1643-keV transitions up to a (tentative) 16^+ state at 8432 keV. In Ref. [20] the 1419-keV transition between the (10^+) and 8^+ states was found to be bypassed by a cascade of 765-, and 998-keV transitions, making the 998-keV line a doublet. The 403-keV gate shows peaks at 765, 998, and 1345 keV. The 1419-keV transition is not seen with this gate, but instead a peak at 1409 keV is observed, which appears to be a new transition in ^{70}Br.

With the 403-keV gate the linking transitions from Band 1 and Band 2 are seen. The 695- and 666-keV transitions were observed in the both previous works, but the 597-keV transition was only observed in Ref. [14]. The spectrum gated with the 403-keV transition shows additionally peaks at 610, 798, 818, and 1104 keV. The 610-, 798-, and 818-keV γ rays have not been previously assigned to ^{70}Br, while the 1104-keV transition was previously observed only in Ref. [14] and was assigned to feed the 1658-keV, 5^+ state.

Figure 4(b) shows the coincident γ rays with the 321-keV gate. Some coincidences are again observed with unknown transitions, with energies of 464-, 610-, and 818-keV. As the 610- and 818-keV transitions were also observed with the 934-keV gate (in addition to the 403-keV gate), these
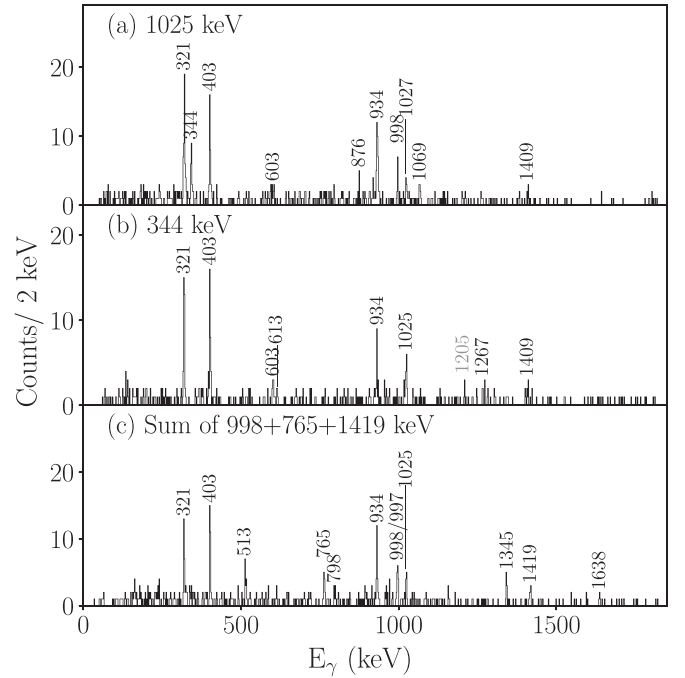
transitions are assigned to feed the 1658-keV, 5^+ state. Even if the 464-keV transition is seen more clearly with the 321-keV gate, this transition is not likely feeding a new 1^+ state as there are no signs of 873-keV γ-ray transition in Fig. 4(b). Therefore, the 464-keV transition is assigned to feed the 1658-keV, 5^+ state. The assignment of the 1104-keV transition is the same as made in Ref. [14], but since also a weak 1104-to 886-keV coincidence was observed in the present analysis, the 886-keV transition is assigned to feed the 2762-keV state.

Figure 4(c) shows the sum of gates on the 321- and 403-keV γ rays. The high-energy part shows peaks at 1345 and 1638 keV, which are believed to be the same ones as observed in Ref. [20], de-exciting the 6788-keV (14^+) and 8426-keV (16^+) states, respectively. No evidence of 1419-keV transition is seen with the sum of 321- and 403-keV gates, so the de-excitation path from the 4446-keV (10^+) state seems to favor the 765-998 cascade, which goes through a 3682-keV (8^+) state.

Figure 5(a) shows the coincident γ rays with the 1025-keV transition, which de-excites the 2683-keV 7^+ state. Strong coincidences with the main cascade containing the 934-, 403-, 321-, and 344-keV transitions are seen. This gate shows also the 998-keV transition, which feeds the 7^+ state at 2683 keV from the 3682-keV (8^+) state. The 765-keV transition feeding the 3682-keV (8^+) state is not apparent in this particular spectrum but becomes visible with a more relaxed β-energy gate. With the 1025-keV gate, a peak at 1409 keV is again observed, while a new peak at 603 keV appears.

Figure 5(b) shows coincidences with the 344-keV γ-ray transition, which de-excites the 8^+ state at 3027 keV and feeds the 2683-keV 7^+ state. The 934-, 403-, 321-, and 1025-keV transitions lying below the 2683-keV state are clearly observed. Since the 1409-keV line is also seen with this gate, it is assigned to feed the 3027-keV 8^+ state from a new state at 4436 keV. The new 603-keV transition is also seen here, which suggests it is feeding the 3027-keV state. Another new γ-ray transition is observed at 1267-keV, which increments with the sum of the 344-1025-keV gates. Therefore, the 1267-keV transition is assigned to feed the 3027-keV state as well.

The nonobservation of the 765-998-keV cascade with the 344-keV gate confirms its placement made previously in Ref. [20]. However, since the 1419-keV transition, which was proposed in Ref. [20] to feed the 3027-keV state, is not observed with any of the previous gates, the intensity of this transition must be significantly lower in the present study than quoted in Ref. [20]. The reason for this might be related to the different fusion-evaporation reactions used here [^{40}Ca(^{32}S, pn) ^{70}Br] and in Ref. [20] [^{40}Ca(^{36}Ar, αpn) ^{70}Br], and, therefore, the population of the excited states and the observed feeding paths can demonstrate significant differences.

Figure 5(c) shows the coincidences with the sum of gates on the 998/997-, 765-, and 1418-keV transitions. The coincidences with the γ rays at 934, 321, 403, and 1025 keV de-exciting the connected states below the 2683-keV state are apparent. This spectrum shows also peaks at 1418, 997, 1345, and 1638 keV, which likely correspond to the 1419-997-1345-1643-keV cascade between the 3028-keV 8^+ and 8432-keV (16^+) states observed in Ref. [20].

Peaks at 513 and 798 keV are likely new transitions in ^{70}Br. The 513-keV transition is tentatively assigned to feed the 4446-keV (10^+) state, while the 798-keV transition is tentatively assigned to feed the 3682-keV (8^+) state based on the coincidences seen with the individual gates on the 765- and 998/997-keV transitions.

The previously observed 391- and 735-keV γ rays from the 2683- and 3027-keV states are not observed in the co-incidences of Band 3 as these transitions are feeding the long-lived 9^+ isomer, which is discussed in more detail in Sec. III D.

D. Band 4

The β-decaying isomeric 9^+ state in ^{70}Br was first reported in Ref. [33]. The excitation energy of the isomer was established in Ref. [20], in addition to the observation of excited states lying above the 9^+ state. The decay energy Q_{EC} of the isomer was reported to be 12.19($\pm 7_{stat}$, $\pm 4_{sys}$) MeV in Ref. [34]. More recently, the half-life of the isomer was measured to be $t_{1/2} = 2157^{+53}_{-49}$ ms [23].

In the current analysis, an attempt was made to correlate with the high-energy β particles from the decay of the 9^+ isomer in ^{70}Br. The resulting recoil-β tagged JUROGAM 3 singles γ-ray spectrum is shown in Fig. 6. The tagging conditions used recoil-decay correlation search-time window of 400–6000 ms, Tuike β-energy threshold of 5 MeV and JYUTube charged-particle fold less than 2. The random background subtracted from this spectrum is defined to be those
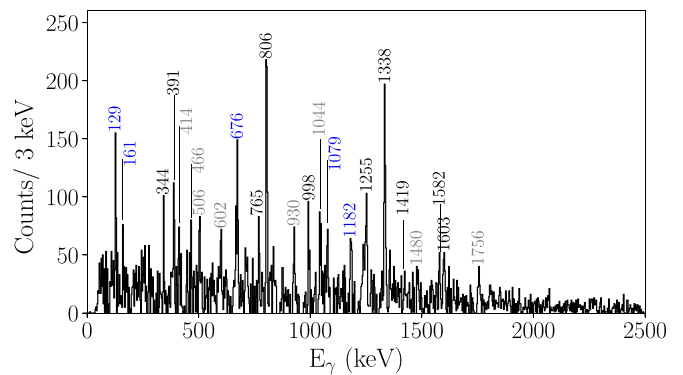

FIG. 6. Recoil-β tagged singles γ-ray spectrum showing transitions connecting to the long-lived 9^+ isomer in ^{70}Br. See text for details. The lines originating from ^{69}Se are marked in blue. The origin of the peaks labeled in gray could not be confirmed in the present analysis.

recoil-β correlations, which do not pass these conditions. Obviously, searching for recoil-decay correlations over several seconds unavoidably leads to significant degree of random correlations (or contamination), which may still be visible in the spectrum even after the background subtraction. Therefore, some caution is required when interpreting the resulting γ-ray spectrum. For example, one of the strongest reaction channels ^{69}Se [$Q_{EC} = 6.68(3)$ MeV, $t_{1/2} = 27.4(2)$ s] can be expected to be present in the tagged spectrum. In the current work the tagged spectrum is simply compared to the previously made assignments for ^{70}Br in Ref. [20] and the level ordering above the 9^+ isomer shown in Fig. 1 is directly adopted from that work for those transitions seen also in the current work. However, re-ordering of the γ rays in Band 4 can be speculated based on the observed γ-ray intensities and the newly identified 603- and 1409-keV transitions.

In Fig. 6, the most intense γ-ray peaks are observed at 806 and 1338 keV. Both of these transitions have been previously placed above the 9^+ isomer in ^{70}Br [20]. Additionally, γ-ray transitions at 1255, 1582, and 1603 keV are observed, which are proposed to form a cascade with the 1338-keV transition in Ref. [20]. This observation indicates, that there is still some sensitivity to correlate with long-lived, but high-energy β decays. Comparison of the 1338- and 1255-keV transition intensities suggests that these transitions are the other way around.

In Fig. 6, a peak at 391 keV can be seen. In Ref. [20] this transition was assigned to connect the Band 3 from the 7^+ state at 2683 keV to the 9^+ state. Additionally, peaks at 344, 765, 998, and 1419 keV can be seen in Fig. 6, which are also observed in the fast 0^+ ground-state β-decay correlated spectra. This observation confirms the structure of Band 3 and unambiguously fixes the excitation energy of the isomeric 9^+ state in ^{70}Br.

Interestingly, the observed strong 806-keV transition was suggested in Ref. [20] to connect a 1433-, 1520-, 1662-, and 1795-keV even-spin cascade to the 9^+ state. In Fig. 6, no clear signs of any of these transitions are seen. This observation raises some questions about the validity of the proposed band.

The peaks at 129, 161, 676, 1079, and 1182 keV are γ-ray transitions from ^{69}Se [35]. The observed 603-keV peak is probably the same transition as discussed in Sec. III C. If the 1338- and 1255-keV transitions were interchanged, as suggested by the intensity balance, the 603-keV peak would fit between the resulting 3630-keV state in the isomer band and the 3027-keV state in Band 3. Moreover, if the 806-keV state would be placed to feed the assumed 3630-keV state in the isomer band, then the newly observed 1409-keV transition connecting to Band 3 (see Sec. III C) would fit between the assumed 4436- and 3027-keV states. However, this scenario cannot be confirmed with certainty in the current analysis.

The other peaks at 414, 506, 930, 1044, 1480, and 1756 keV could not be associated with any contaminant nuclei. It is therefore possible that these transitions are lying above the 9^+ state in ^{70}Br.

IV. RESULTS FOR THE $N = Z - 2$ NUCLEUS ^{70}Kr

The level structure of ^{70}Kr has been studied earlier at JYFL-ACCLAB using the RITU gas-filled separator and the JUROGAM 2 Germanium-detector array [8]. The γ rays with energies of 870(1) keV and 997(1) keV were tentatively assigned to represent the $2^+ \longrightarrow 0^+$ and $4^+ \longrightarrow 2^+$ transitions in ^{70}Kr, respectively. More recently, the excited states in ^{70}Kr have been populated using one- and two-neutron removal and inelastic scattering reactions at RIKEN [13]. According to the experiment reported in Ref. [13], the γ-ray energies of the $2^+ \longrightarrow 0^+$ and $4^+ \longrightarrow 2^+$ transitions in ^{70}Kr were measured to be 884(4_{stat})(5_{sys}) keV and 1029(14_{stat})(5_{sys}) keV, respectively. Hence, there is an apparent disagreement between the two recent experimental results on ^{70}Kr.

Figure 7(a) shows recoil-β tagged JUROGAM 3 γ-ray spectrum with 240-ms correlation search time, 5- to 10-MeV β-energy gate and with a condition that exactly one charged particle was detected in the JYUTube scintillator detector. The resulting γ-ray spectrum shows the known transitions originating from ^{70}Br (red labels) and ^{66}As (blue labels). Figure 7(b) is similar to Fig. 7(a), but uses shorter correlation time of 90 ms, and a condition that zero charged particles were detected in JYUTube. These correlation conditions are suitable for ^{70}Kr as this nucleus is produced in the $2n$ evaporation channel and the ground-state β-decay half-life is $t_{1/2} = 45.19(14)$ ms [19]. The resulting spectrum is still dominated by the ^{70}Br (pn) and ^{66}As (αpn) γ-ray transitions as the JYUTube veto efficiency for one proton is limited to approximately 70%. However, the spectrum shown in Fig. 7(b) reveals a clear γ-ray peak at 881(1) keV, and a weaker one at 1037(2) keV, which could potentially be associated with ^{70}Kr. The energy regions at 881 and 1037 keV are indicated in the Fig. 7(a) as dashed vertical lines, but no signs of clear γ-ray peaks are observed there.

To unambiguously identify the γ-ray transitions originating from the decay of the excited states in ^{70}Kr, the recoil-$\beta - \beta$ correlation method was employed in the current analysis. The recoil-double-β tagging (RDBT) technique was recently applied for the first time to identify γ-ray transitions in ^{62}Ge [21]. Further details about the technique will be
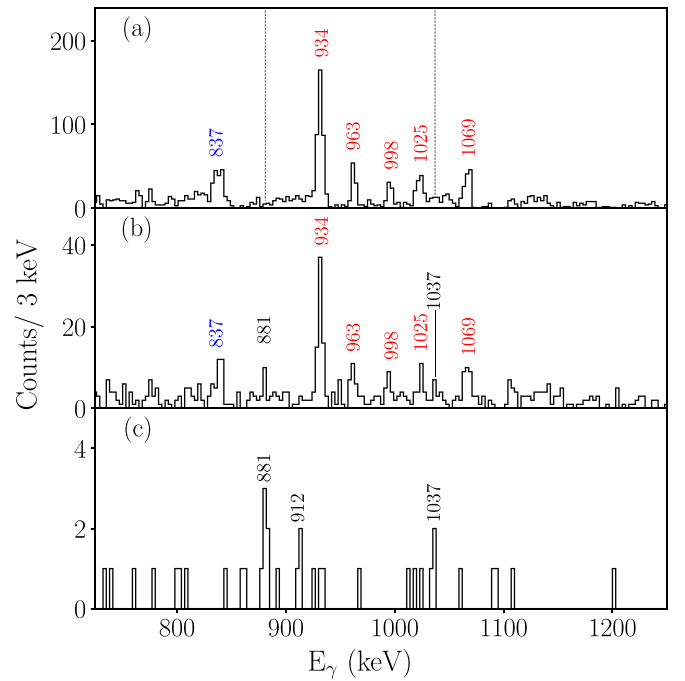

FIG. 7. Recoil-β tagged JUROGAM 3 γ-ray spectra with 5- to 10-MeV β-energy gate, and using (a) search time of 240 ms, and a condition that exactly one charged particle was detected in JYUTube, and (b) search time of 90 ms, and requiring detection of zero charged particles in JYUTube. (c) Recoil-$\beta - \beta$ tagged JUROGAM 3 γ-ray spectrum with zero charged particles detected in JYUTube, and using 150-ms and 300-ms correlation search times, and 1- to 10-MeV β-energy gates for the first and second β decays, respectively. The γ rays labeled in blue and red are known transitions in ^{66}As and ^{70}Br, while the transitions labeled in black are associated with ^{70}Kr. The dashed vertical lines in panel (a) indicate the locations of the 881- and 1037-keV γ-ray peaks observed in panels (b) and (c).

presented in the forthcoming publication focusing on the $A = 78$ triplet [36].

In the present case, the 45.19(14)-ms [19], ^{70}Kr $\longrightarrow$ ^{70}Br β decay, followed by the 78.42(51)-ms [23], ^{70}Br $\longrightarrow$ ^{70}Se β decay provides a clean tag for the identification of γ rays originating from ^{70}Kr. This method has been applied in Fig. 7(c), where, in addition to the charged-particle veto and set β-energy gates of 1–10 MeV for both decays, the correlation times for the first and second β decays are 150 and 300 ms, respectively. As can be observed in Fig. 7(c), the RDBT method yields six γ-ray events at 881(1) keV, three events at 1037 keV and three events at 912 keV. If using more restrictive β-energy gates of 2–10 MeV for both decays, then two events are left in the 881-keV peak, but the other two peaks disappear. Nevertheless, since the same γ-ray transitions at 881(1) keV and 1037(2) keV are clearly observed in both Figs. 7(b) and 7(c), these transitions are assigned as the $2^+ \longrightarrow 0^+$ [881(1) keV] and tentatively as the $4^+ \longrightarrow 2^+$ [1037(2) keV] transitions in ^{70}Kr. The third peak at 912(2) keV in Fig. 7(c), could in principle represent the $6^+ \longrightarrow 4^+$ transition in ^{70}Kr. This scenario is supported by the comparison to the other members of the $A = 70$ triplet, where the analog transitions in ^{70}Se and ^{70}Br are 964 and

963 keV, respectively. However, this assignment needs to be confirmed in future experiments.

The observed 881(1)- and 1037(2)-keV γ-ray transitions are in agreement within the uncertainties with the 884(4_{stat})(5_{sys})-keV, $2^+ \longrightarrow 0^+$ and 1029(14_{stat})(5_{sys})-keV, $4^+ \longrightarrow 2^+$ transitions reported in Ref. [13], which increases the confidence of the assignments of these transitions. Lastly, the γ-ray energies measured in the current work provide more accurate excitation energy values for the 2^+ and 4^+ states in ^{70}Kr.

V. DISCUSSION

The ^{70}Br levels and their configurations have been extensively discussed and interpreted in terms of various theoretical models in Ref. [20]. The findings were that the low-lying states in ^{70}Br are associated with pf configurations with modest axially symmetric deformation, while the isomeric structure was interpreted to be based on the coupling of the odd proton and odd neutron in the $g_{9/2}$ orbital to a well-deformed oblate core. In Ref. [20] the strong cascade based on the 1337-keV 3^+ state (Band 3 in the current work) did not receive that much attention so one qualitative observation will be presented here.

In ^{62}Ga the high-spin part of the experimentally observed strong $T = 0$ band from the 9^+ state up to the terminating 17^+ state can be viewed as coupling the ground-state band of ^{60}Zn to a np pair in the $g_{9/2}$ orbital. In Ref. [37] it was pointed out that the ground-state band in ^{60}Zn (the cascade with $0^+ - 8^+$) show marked similarity with the $9^+ - 17^+$ cascade in ^{62}Ga in terms of the transition energies, in addition to the observed backbending and band termination. The question is if ^{70}Br structures show similar behavior, i.e., coupling of the isoscalar np pair in the $g_{9/2}$ orbital ($I = 9$) to the ground-state band of ^{68}Se. The obvious candidate in ^{70}Br is the band based on the 9^+ isomer (Band 4), but this band is having clearly different moment of inertia in comparison to the ground-state band of ^{68}Se. The isomer-based band is perhaps more similar to the excited prolate band in ^{68}Se starting at an excitation energy of 1594 keV [38].

Interestingly, the 765-997-1345-1638–keV sequence in Band 3 of ^{70}Br is much closer to the 853-1088-1362-1567–keV cascade observed in ^{68}Se, with almost identical kinematic moment of inertia. The ground-state band in ^{68}Se has been interpreted to result from rotation of an oblate deformed system [38]. However, the tentative spin assignment of the 3682-keV state in ^{70}Br is 8^+, instead of 9^+, and also the other higher-lying states in this cascade have been tentatively assigned even spins in Ref. [20]. If the band head is truly 8^+, then this structure could be associated with isovector coupling of the $g_{9/2}$ neutron and proton ($I = 8$) to the ^{68}Se core. This scenario would explain the relatively high excitation energy (3682 keV) of the band-head state with respect to the 9^+ isomeric state. The energy difference between the isoscalar and isovector couplings was investigated in Ref. [39] to be about 2 MeV in the case of ^{66}As.

Different spin assignments for the 3682-8426–keV states cannot be fully excluded as the assignments made in Ref. [20] are tentative. The $9^+ - 17^+$ assignment would actually make the band closer to the yrast line and therefore favor its population. Also, the angular correlation analysis made for the 998/997-keV doublet indicates a quadrupole character for both transitions. However, the 998-keV transition, considering the suggested spin assignments (8^+ for the 3682-keV state, and 7^+ for the 2683-keV state) should be a dipole. Moreover, the observed weak intensity of the 1419-keV transition in the current work could then be explained by its potential $M3$ character, if the state at 4446 keV would be 11^+ rather than 10^+. To clarify the situation, the spin-parities in Band 3 would therefore need a rigorous experimental confirmation, in addition to a detailed theoretical examination of the proposed scenario.

A. Shell-model calculations for ^{70}Kr, ^{70}Br, and ^{70}Se

The new shell-model calculations presented here for the $A = 70$ triplet have been performed using the code KSHELL [40]. The ^{56}Ni nucleus was considered as a closed inert core with protons and neutrons in the valence space spanned by the $0f_{5/2}$, $1p_{3/2}$, $1p_{1/2}$, and $0g_{9/2}$ orbitals. The effective two-body Hamiltonian (H^{eff}), already adopted in the several previous studies [41–43], was derived within the framework of many-body perturbation theory, starting from the CD-Bonn nucleon-nucleon potential [44] renormalized by the V_{low-k} approach with the addition of the Coulomb term for the proton-proton interaction. In particular, the two-body matrix elements have been calculated within the $\hat{Q}$-box folded-diagram approach [45], including the perturbative expansion of the $\hat{Q}$-box one- and two-body diagrams up to the third order in the interaction. The single-particle energies were taken from the experiments as was done in Ref. [43], except for the $0g_{9/2}$ orbital, whose energy was fixed to 3.2 MeV for both protons and neutrons. This gives the theoretical spectra of nuclei in this region in reasonably good agreement with the experimental data, as discussed in Ref. [42].

For the calculation of the collective properties of nuclei in the shell-model approach, such as the spectroscopic quadrupole moments (Q_s), the contributions arising from the configurations outside the chosen shell-model valence space need to be compensated by the use of effective transition operators and effective charges. The effective $E2$ operators were calculated within the same framework of the shell-model Hamiltonian, by employing the Suzuki-Okamoto formalism [46]. The effective charges obtained for the $E2$ operator are state dependent, ranging from $1.3e$ to $1.8e$ for protons and $0.8e$ to $1.4e$ for neutrons.

Figure 8 shows the shell-model calculated spectroscopic quadrupole moments [Q_s (efm^2)] as a function of spin for the low-lying $T = 1$ states in ^{70}Kr, ^{70}Br, and ^{70}Se. The predicted positive and negative Q_s values indicate oblate and prolate shapes for these states, respectively. The striking feature of these results is that there is no shape change predicted between the members of the $A = 70$ triplet, but on the other hand a sudden jump from oblate deformation at spin 6^+ to prolate deformation at spin 8^+. The oblate shape for the 2_1^+ state in ^{70}Se has been experimentally established based on the combined Coulomb excitation and lifetime measurements presented in Refs. [47,48].
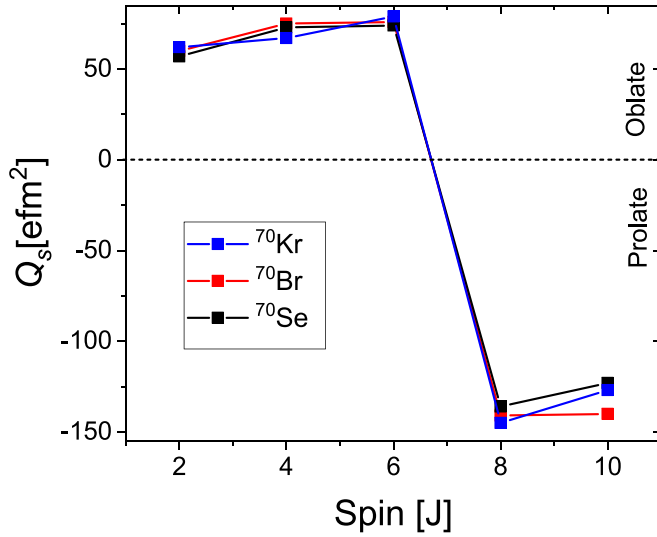
FIG. 8. Spectroscopic quadrupole moments obtained from the shell-model calculations as a function of spin for the low-lying $T = 1$ states in ^{70}Kr, ^{70}Br, and ^{70}Se [50].

FIG. 9. Coulomb energy differences between the isobaric analog states in ^{70}Br and ^{70}Se as a function of the spin (J). Experimental CED data are shown in red, present shell-model calculation in black and calculations by Kaneko *et al.*, in blue (obtained from Ref. [6]).

The lifetime of the 2_1^+ state in ^{70}Br was reported in Ref. [49]. This work concluded that the level of collectivity for the $2_1^+ \longrightarrow 0_{gs}^+$ transitions is similar in ^{70}Br and ^{70}Se, indicating that there is no major shape change at low spin between these nuclei. These results were recently confirmed in the inelastic scattering experiment of Ref. [16], which yielded similar $B(E2; 0^+ \longrightarrow 2^+)$ values for ^{70}Br and ^{70}Se as were found in Ref. [49]. The shell-model results presented in Fig. 8 are therefore in line with the experimental observations for ^{70}Br and ^{70}Se. Moreover, in Ref. [48] it was concluded that the ground state band in ^{70}Se stays oblate up to the 4^+ state, but then turns into prolate at the 6^+ state, which is in contrast with the current calculation.

For ^{70}Kr the situation is somewhat unclear since the recently measured $B(E2; 0^+ \longrightarrow 2^+)$ value suggests a major shape change, presumably to prolate deformation, but the present calculation or the ones presented in Ref. [16] do not support this scenario. In the present analysis no new low-lying states below the 934-keV, 2^+ state in ^{70}Br could be identified with certainty, which would support the argument raised in Ref. [17] as a solution for the observed isospin symmetry breaking implied by the experimental data of Ref. [16]. In addition, a recent work presented in Ref. [19], investigated ^{70}Kr β decay into excited states in ^{70}Br and reported on a new 1^+ state (among other new 1^+ and 0^+ states) at 1120 keV. The population of this state was not observed in the current study.

B. Coulomb, mirror, and triplet energy differences for the $A = 70$, $T = 1$ triplet

The present work confirms the unique negative CED behavior only observed in the mass $A = 70$ pair in the $A = 60$–80 mass region [3,6,7,9,14]. The typically positive CED trends are attributed to result from the interplay of Coulomb multipole effects and the alignment of valence nucleons with the increasing angular momentum [1]. Particularly, the
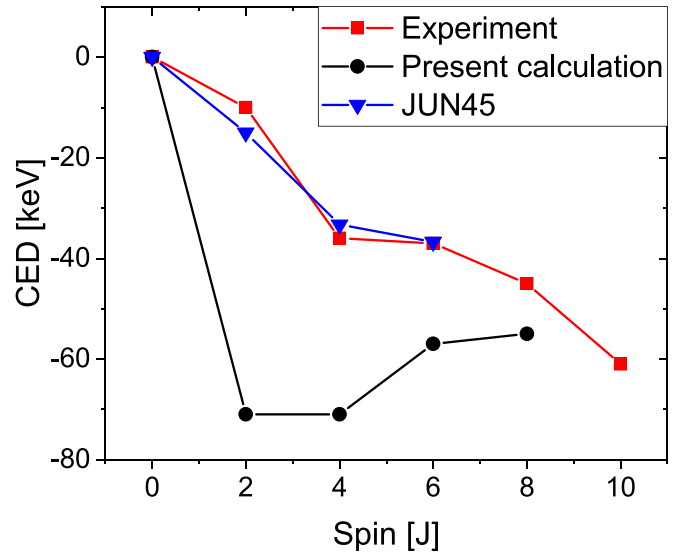
alignment of the proton-proton (pp) pairs causes reduction in the Coulomb energy of a state as the spatial overlap of the proton wave functions decreases. Since the number of active pp pairs in the $N = Z$ nucleus can be expected to be lower than in the $N = Z + 2$ neighbor, the analog states in the $N = Z$ member should correspondingly have larger excitation energies causing a positive CED trend.

In Ref. [14] the compression of the level energies in ^{70}Br in comparison to ^{70}Se, leading to the unique negative CED at $A = 70$ was suggested to be related to the increased proton radius for drip-line nuclei in two ways. Firstly, the spatial expansion of the proton wave function causes reduction in the Coulomb energy, similar to the mechanism in Thomas-Ehrman shift. Secondly, the two-body residual interaction is decreased due to the reduced overlap of neutron and loosely bound proton radial wave functions. However, these kind of effects would also be expected to be seen in the other medium-heavy $N = Z$ systems. An alternative explanation was given in Ref. [3], where the anomalous negative CED at $A = 70$ was attributed to the possible shape changes between ^{70}Br and ^{70}Se. A similar conclusion was reached in Ref. [15], where the complex excited VAMPIR calculations predicted different shape mixing behavior of the ^{70}Br and ^{70}Se excited states—the oblate shapes were found to be more dominant in ^{70}Se than in ^{70}Br. Obviously, this interpretation stands in contrast to the experimental evidence for the similar oblate shapes in ^{70}Se and ^{70}Br at low spin, as discussed in the previous section.

The third explanation for the negative CED in the $A = 70$ pair has been proposed in Ref. [6]. In this work, the shell-model calculations were carried out by using the JUN45 effective interaction [51] in the $pf_{5/2}g_{9/2}$ model space. These calculations, shown also in Fig. 9 as blue triangles, reproduce the CED correctly up to the $J^{\pi} = 6^+$ state with nearly static oblate deformation for ^{70}Se (and presumably for ^{70}Br as well).

TABLE II. Experimental mirror and triplet energy differences for the 2^+ and 4^+ states in the mass $A = 70$ triplet compared to the predictions obtained from theoretical calculations. The shell-model calculations with (w) and without (w/o) the INC interaction that are obtained from Ref. [7] are labeled with,[a] and the present shell-model calculations are labeled with.[b]

I^π	$E_{\text{level}}^{\text{exp}}$ (keV)	Exp (keV)		SM (keV)[a]				SM (keV)[b]	
		MED	TED	MED w INC	MED w/o INC	TED w INC	TED w/o INC	MED	TED
2^+	870[a]	−74.5	−53.5	−70	−50	−68	−24	−145	−3
	884(4)(5)[b]	−60	−39.5						
	881(1)[c]	−64.5	−43.5						
4^+	1867[a]	−171	−100	−132	−90	−116	−48	−150	−36
	1913(14)(5)[b]	−125	−54.2						
	1917(2)[c]	−123.8	−52.2						

[a]From Debenham *et al.* [8].
[b]From Wimmer *et al.* [13].
[c]Current work.

The negative CED is attributed to the enhanced neutron excitations (and reduced proton excitations) from the fp shell to the $g_{9/2}$ orbital due to the electromagnetic spin-orbit interaction, which alters the neutron and proton single-particle orbitals in opposite direction. It should be emphasized, that this calculation did not incorporate any additional INC interaction.

The CED results from the present shell-model calculation are shown in Fig. 9 as black circles. The calculation seems to correctly reproduce the negative CED trend with similar deformations for ^{70}Br and ^{70}Se, so the shape evolution does not appear to be the leading cause of the CED behavior at $A = 70$ (see Figs. 8 and 9). However, the CED magnitude is clearly overestimated, especially at $J^\pi = 2^+$. The overestimation may be caused by the uncertainty on the single-particle energies of the $g_{9/2}$ orbital or by the two body-effective interaction. Therefore, an experimental indication on the single-particle energy of the $g_{9/2}$ orbital would be important to shed light on the problem. This can be obtained, for example, extracting nucleon occupancies from nucleon-adding and -removing reactions as done for example in Refs. [52–54] and compare them with theoretical data extracted from shell-model calculations. Lastly, for the used interaction H^{eff} it is not possible to single out additional INC terms and obviously those should not be needed here.

In Table II, the experimental MED and TED values for the 2^+ and 4^+ states are compared to the shell-model predictions obtained from Ref. [7], which employs the JUN45 interaction and to the present calculations. For the sake of completeness, the experimental data includes also the different results from Refs. [8,13], in addition to the results obtained in the present work. In Ref. [7], the calculation used an additional INC interaction, which was adjusted to reproduce the experimental MED and TED data for $A = 66$. The INC interaction was divided into the isotensor ($\beta_{(2)}^{J=0} = \beta_{pp} + \beta_{nn} - 2\beta_{pn}$) and isovector ($\beta_{(1)}^{J=0} = \beta_{pp} - \beta_{nn}$) components with strengths of $+100$ keV and $+300$ keV, respectively. It should be noted that the need for the additional isotensor INC term for $J = 0$, with a universal strength of about $+100$ keV was also demonstrated in Ref. [55] in order to reproduce the experimental TED data in a wide mass range of $A = 18-66$.

If the TED predictions from Ref. [7] are compared to the new experimental TED values (-43.5 keV at 2^+, -52.2 keV at 4^+), the agreement with theory is actually better without the INC interaction (-24 keV at 2^+, -48 keV at 4^+) as opposed to with it (-68 keV at 2^+, -116 keV at 4^+). This observation is clearly in contradiction with the conclusion that the isotensor INC term is globally required for the reproduction of the TED magnitude. Interestingly, the same is not true for MED as the experimental values (-64.5 keV at 2^+, -123.8 keV at 4^+) agree better with the shell-model calculation of Ref. [7], where the INC correction has been incorporated (-70 keV at 2^+, -132 keV at 4^+). The new shell-model results can only qualitatively reproduce the correct signs of TED and MED - TED is underestimated by 40 and 20 keV, while MED is overestimated by 80 and 30 keV for the 2^+ and 4^+ states, respectively. On the other hand, this can still be considered as a satisfactory result, considering that the model does not use other adjustable parameters in addition to the neutron and proton single-particle energies, which are (for the most part) based on experiment. However, taking also into account the clear overestimation of CED, it seems that the calculation is overestimating the excitation energies for ^{70}Se and, therefore, the neutron single-particle energies should perhaps be reevaluated to reach a better agreement with experiment.

Based on this discussion, the degree to which the INC interaction demonstrate consistency across the different mass regions starts to look somewhat uncertain. Consequently, further theoretical investigations of these new experimental results are encouraged to be pursued in order to resolve the long-standing question if the INC interaction has a nuclear structure origin.

VI. CONCLUSION

In summary, the excited states in the ^{70}Kr and ^{70}Br members of the $A = 70$, $T = 1$ isospin triplet have been investigated employing the selective recoil-β and recoil-β-β tagging methods. The $T = 1$ band in ^{70}Br was extended (tentatively) up to $J^\pi = 10^+$, while the discrepancy on the excitation energies of the 2^+ and 4^+ states in ^{70}Kr was settled. These results allowed the comparison of the excitation energy differences of the isobaric analog states in the $A = 70$

triplet and yielded experimental CED, MED, and TED values. The experimental CED, MED, and TED values were compared against two independent shell-model calculations. The confirmed unique negative CED trend for the ^{70}Br and ^{70}Se pair could not be associated with the nuclear shape changes. The role of the isospin symmetry nonconserving interaction remains unclear in this mass region, since the comparisons of the experimental MED and TED values to the shell-model predictions are contradictory.

The experimental data for this article, and the corresponding metadata, are stored in the Finnish national FAIRdata repository and available from Ref. [56].

[1] M. Bentley and S. Lenzi, Prog. Part. Nucl. Phys. **59**, 497 (2007).

[2] P. E. Garrett, W. E. Ormand, D. Appelbe, R. W. Bauer, J. A. Becker, L. A. Bernstein, J. A. Cameron, M. P. Carpenter, R. V. F. Janssens, C. J. Lister, D. Seweryniak, E. Tavukcu, and D. D. Warner, Phys. Rev. Lett. **87**, 132502 (2001).

[3] B. S. Nara Singh, A. N. Steer, D. G. Jenkins, R. Wadsworth, M. A. Bentley, P. J. Davies, R. Glover, N. S. Pattabiraman, C. J. Lister, T. Grahn, P. T. Greenlees, P. Jones, R. Julin, S. Juutinen, M. Leino, M. Nyman, J. Pakarinen, P. Rahkila, J. Sarén, C. Scholey *et al.*, Phys. Rev. C **75**, 061301(R) (2007).

[4] S. M. Lenzi, N. Mărginean, D. R. Napoli, C. A. Ur, A. P. Zuker, G. de Angelis, A. Algora, M. Axiotis, D. Bazzacco, N. Belcari *et al.*, Phys. Rev. Lett. **87**, 122501 (2001).

[5] M. A. Bentley, S. M. Lenzi, S. A. Simpson, and C. A. Diget, Phys. Rev. C **92**, 024310 (2015).

[6] K. Kaneko, T. Mizusaki, Y. Sun, S. Tazaki, and G. de Angelis, Phys. Rev. Lett. **109**, 092504 (2012).

[7] K. Kaneko, Y. Sun, T. Mizusaki, and S. Tazaki, Phys. Rev. C **89**, 031302(R) (2014).

[8] D. M. Debenham, M. A. Bentley, P. J. Davies, T. Haylett, D. G. Jenkins, P. Joshi, L. F. Sinclair, R. Wadsworth, P. Ruotsalainen, J. Henderson, K. Kaneko, K. Auranen, H. Badran, T. Grahn, P. Greenlees, A. Herzáář, U. Jakobsson, J. Konki, R. Julin, S. Juutinen *et al.*, Phys. Rev. C **94**, 054311 (2016).

[9] P. Ruotsalainen, C. Scholey, R. Julin, K. Hauschild, K. Kaneko, B. S. Nara Singh, R. Wadsworth, D. G. Jenkins, T. S. Brock, P. T. Greenlees, J. Henderson, U. Jakobsson, P. Jones, S. Juutinen, S. Ketelhut, M. Leino, N. M. Lumley, P. J. R. Mason, P. Nieminen, M. Nyman *et al.*, Phys. Rev. C **88**, 024320 (2013).

[10] J. Henderson, D. G. Jenkins, K. Kaneko, P. Ruotsalainen, P. Sarriguren, K. Auranen, M. A. Bentley, P. J. Davies, A. Görgen, T. Grahn, P. T. Greenlees, A. Hay, T. W. Henry, A. Herzáář, U. Jakobsson, R. Julin, S. Juutinen, J. Konki, M. Leino, C. McPeake *et al.*, Phys. Rev. C **90**, 051303(R) (2014).

[11] E. Bouchez, I. Matea, W. Korten, F. Becker, B. Blank, C. Borcea, A. Buta, A. Emsallem, G. de France, J. Genevey, F. Hannachi, K. Hauschild, A. Hürstel, Y. Le Coz, M. Lewitowicz, R. Lucas, F. Negoita, F. de Oliveira Santos, D. Pantelica, J. Pinston *et al.*, Phys. Rev. Lett. **90**, 082502 (2003).

[12] G. de Angelis, K. T. Wiedemann, T. Martinez, R. Orlandi, A. Petrovici, E. Sahin, J. J. Valiente-Dobón, D. Tonev, S. Lunardi, B. S. Nara Singh, R. Wadsworth, A. Gadea, K. Kaneko, P. G. Bizzeti, A. M. Bizzeti-Sona, B. Blank, A. Bracco, M. P. Carpenter, C. J. Chiara, E. Farnea *et al.*, Phys. Rev. C **85**, 034320 (2012).

[13] K. Wimmer, W. Korten, T. Arici, P. Doornenbal, P. Aguilera, A. Algora, T. Ando, H. Baba, B. Blank, A. Boso, S. Chen, A. Corsi, P. Davies, G. de Angelis, G. de France, D. Doherty, J. Gerl, R. Gernhäuser, D. Jenkins, S. Koyama *et al.*, Phys. Lett. B **785**, 441 (2018).

[14] G. de Angelis, T. Martinez, A. Gadea, N. Marginean, E. Farnea, E. Maglione, S. Lenzi, W. Gelletly, C. A. Ur, D. R. Napoli, T. Kroell, S. Lunardi, B. Rubio, M. Axiotis, D. Bazzacco, A. M. B. Sona, P. G. Bizzeti, P. Bednarczyk, A. Bracco, F. Brandolini *et al.*, Eur. Phys. J. A **12**, 51 (2001).

[15] A. Petrovici, Phys. Rev. C **91**, 014302 (2015).

[16] K. Wimmer, W. Korten, P. Doornenbal, T. Arici, P. Aguilera, A. Algora, T. Ando, H. Baba, B. Blank, A. Boso, S. Chen, A. Corsi, P. Davies, G. de Angelis, G. de France, J.-P. Delaroche, D. T. Doherty, J. Gerl, R. Gernhäuser, M. Girod *et al.*, Phys. Rev. Lett. **126**, 072501 (2021).

[17] S. M. Lenzi, A. Poves, and A. O. Macchiavelli, Phys. Rev. C **104**, L031306 (2021).

[18] H. David, P. Woods, G. Lotay, D. Seweryniak, M. Albers, M. Alcorta, M. Carpenter, C. Chiara, T. Davinson, D. Doherty, C. Hoffman, R. Janssens, T. Lauritsen, A. Rogers, and S. Zhu, Phys. Lett. B **726**, 665 (2013).

[19] A. Vitéz-Sveicicer, A. Algora, A. Morales, B. Rubio, G. Kiss, P. Sarriguren, P. Van Isacker, G. de Angelis, F. Recchia, S. Nishimura, J. Agramunt, V. Guadilla, A. Montaner-Pizá, S. Orrigo, A. Horváth, D. Napoli, S. Lenzi, A. Boso, V. Phong, J. Wu *et al.*, Phys. Lett. B **830**, 137123 (2022).

[20] D. G. Jenkins, N. S. Kelsall, C. J. Lister, D. P. Balamuth, M. P. Carpenter, T. A. Sienko, S. M. Fischer, R. M. Clark, P. Fallon, A. Görgen, A. O. Macchiavelli, C. E. Svensson, R. Wadsworth, W. Reviol, D. G. Sarantites, G. C. Ball, J. Rikovska Stone, O. Juillet, P. Van Isacker, A. V. Afanasjev *et al.*, Phys. Rev. C **65**, 064307 (2002).

[21] K. Wimmer, P. Ruotsalainen, S. Lenzi, A. Poves, T. Hüyük, F. Browne, P. Doornenbal, T. Koiwai, T. Arici, K. Auranen, M. Bentley, M. Cortés, C. Delafosse, T. Eronen, Z. Ge, T. Grahn, P. Greenlees, A. Illana, N. Imai, H. Joukainen *et al.*, Phys. Lett. B **847**, 138249 (2023).

[22] M. Wang, W. Huang, F. Kondev, G. Audi, and S. Naimi, Chin. Phys. C **45**, 030003 (2021).

[23] A. I. Morales, A. Algora, B. Rubio, K. Kaneko, S. Nishimura, P. Aguilera, S. E. A. Orrigo, F. Molina, G. de Angelis, F. Recchia, G. Kiss, V. H. Phong, J. Wu, D. Nishimura, H. Oikawa, T. Goigoux, J. Giovinazzo, P. Ascher, J. Agramunt, D. S. Ahn *et al.*, Phys. Rev. C **95**, 064327 (2017).

[24] M. Wang, W. Huang, F. Kondev, G. Audi, S. Naimi, and X. Xu, Chin. Phys. C **41**, 030003 (2017).

[25] J. Pakarinen, J. Ojala, P. Ruotsalainen, H. Tann, H. Badran, T. Calverley, J. Hilton, T. Grahn, P. T. Greenlees, M. Hytonen, A. Illana, A. Kauppinen, M. Luoma, P. Papadakis, J. Partanen, K. Porras, M. Puskala, P. Rahkila, K. Ranttila, J. Sarén *et al.*, Eur. Phys. J. A **56**, 149 (2020).

[26] J. Uusitalo, J. Sarén, J. Partanen, and J. Hilton, Acta Phys. Pol. B **50**, 319 (2019).

[27] A. Rogers, J. Giovinazzo, C. Lister, B. Blank, G. Canchel, J. Clark, G. de France, S. Grévy, S. Gros, E. McCutchan, F. de Oliveira Santos, G. Savard, D. Seweryniak, I. Stefan, and J.-C. Thomas, Nucl. Data Sheets **120**, 41 (2014).

[28] H. Joukainen, J. Sarén, and P. Ruotsalainen, Nucl. Instrum. Methods A, **1027**, 166253 (2021).

[29] A. Steer, D. Jenkins, R. Glover, B. Nara Singh, N. Pattabiraman, R. Wadsworth, S. Eeckhaudt, T. Grahn, P. Greenlees, P. Jones, R. Julin, S. Juutinen, M. Leino, M. Nyman, J. Pakarinen, P. Rahkila, J. Sarén, C. Scholey, J. Sorri, J. Uusitalo *et al.*, Nucl. Instrum. Methods A **565**, 630 (2006).

[30] J. Henderson, P. Ruotsalainen, D. G. Jenkins, C. Scholey, K. Auranen, P. J. Davies, T. Grahn, P. T. Greenlees, T. W. Henry, A. Herzáň, U. Jakobsson, P. Joshi, R. Julin, S. Juutinen, J. Konki, M. Leino, G. Lotay, A. J. Nichols, A. Obertelli, J. Pakarinen *et al.*, JINST **8**, P04025 (2013).

[31] G. Rainovski, H. Schnare, R. Schwengner, C. Plettner, L. Käubler, F. Dänau, I. Ragnarsson, J. Eberth, T. Steinhardt, O. Thelen, M. Hausmann, A. Jungclaus, K. P. Lieb, A. Müller, G. de Angelis, A. Gadea, D. R. Napoli, A. Algora, D. G. Jenkins, R. Wadsworth *et al.*, J. Phys. G: Nucl. Part. Phys. **28**, 2617 (2002).

[32] M. Wang, G. Audi, A. H. Wapstra, F. G. Kondev, M. MacCormick, X. Xu, and B. Pfeiffer, Chin. Phys. C **36**, 1603 (2012).

[33] B. Vosicki, T. Björnstad, L. Carraz, J. Heinemeier, and H. Ravn, Nucl. Instrum. Methods **186**, 307 (1981).

[34] M. Karny, L. Batist, D. Jenkins, M. Kavatsyuk, O. Kavatsyuk, R. Kirchner, A. Korgul, E. Roeckl, and J. Żylicz, Phys. Rev. C **70**, 014310 (2004).

[35] I. Stefanescu, J. Eberth, G. de Angelis, N. Warr, G. Gersch, T. Steinhardt, O. Thelen, D. Weisshaar, T. Martinez, A. Jungclaus, R. Schwengner, K. P. Lieb, E. A. Stefanova, D. Curien, and A. Gelberg, Phys. Rev. C **69**, 034333 (2004).

[36] G. L. Zimba, P. Ruotsalainen, D. G. Jenkins, X. P. Lopez, J. Uusitalo, W. Satuła, and R. Wadsworth, First identification of excited states in ^{78}zr and implications for isospin non-conserving forces in nuclei (unpublished).

[37] D. Rudolph, I. Ragnarsson, S. Åberg, C. Andreoiu, M. P. Carpenter, R. M. Clark, J. Ekman, C. Fahlander, R. V. F. Janssens, F. G. Kondev, T. Lauritsen, D. G. Sarantites, D. Seweryniak, and C. E. Svensson, Phys. Rev. C **102**, 014313 (2020).

[38] S. M. Fischer, D. P. Balamuth, P. A. Hausladen, C. J. Lister, M. P. Carpenter, D. Seweryniak, and J. Schwartz, Phys. Rev. Lett. **84**, 4064 (2000).

[39] P. C. Srivastava, S. Åberg, and I. Ragnarsson, Phys. Rev. C **95**, 011303(R) (2017).

[40] N. Shimizu, T. Mizusaki, Y. Utsuno, and Y. Tsunoda, Comput. Phys. Commun. **244**, 372 (2019).

[41] L. Coraggio, L. De Angelis, A. Fukui, A. Gargano, N. Itaco, and F. Nowacki, Phys. Rev. C **100**, 014316 (2019).

[42] M. Rocchini, K. Hadyńska-Klęk, A. Nannini, A. Goasduff, M. Zielińska, D. Testov, T. R. Rodríguez, A. Gargano, F. Nowacki, G. De Gregorio, H. Naïdja, P. Sona, J. J. Valiente-Dobón, D. Mengoni, P. R. John, D. Bazzacco, G. Benzoni, A. Boso, P. Cocconi, M. Chiari *et al.*, Phys. Rev. C **103**, 014311 (2021).

[43] I. Ciraldo *et al.* (For the NUMEN collaboration), Phys. Rev. C **105**, 044607 (2022).

[44] R. Machleidt, Phys. Rev. C **63**, 024001 (2001).

[45] L. Coraggio, A. Covello, A. Gargano, N. Itaco, and T. T. S. Kuo, Ann. Phys. **327**, 2125 (2012).

[46] K. Suzuki and R. Okamoto, Prog. Theor. Phys. **93**, 905 (1995).

[47] A. M. Hurst, P. A. Butler, D. G. Jenkins, P. Delahaye, F. Wenander, F. Ames, C. J. Barton, T. Behrens, A. Bürger, J. Cederkäll, E. Clément, T. Czosnyka, T. Davinson, G. de Angelis, J. Eberth, A. Ekström, S. Franchoo, G. Georgiev, A. Görgen, R.-D. Herzberg *et al.*, Phys. Rev. Lett. **98**, 072501 (2007).

[48] J. Ljungvall, A. Görgen, M. Girod, J.-P. Delaroche, A. Dewald, C. Dossat, E. Farnea, W. Korten, B. Melon, R. Menegazzo, A. Obertelli, P. Orlandi, P. Petkov, T. Pissulla, S. Siem, R. P. Singh, J. Srebrny, C. Theisen, C. A. Ur, J. J. Valiente-Dobón *et al.*, Phys. Rev. Lett. **100**, 102502 (2008).

[49] A. Nichols, R. Wadsworth, H. Iwasaki, K. Kaneko, A. Lemasson, G. de Angelis, V. Bader, T. Baugher, D. Bazin, M. Bentley, J. Berryman, T. Braunroth, P. Davies, A. Dewald, C. Fransen, A. Gade, M. Hackstein, J. Henderson, D. Jenkins, D. Miller *et al.*, Phys. Lett. B **733**, 52 (2014).

[50] D. Giovanni (private communication).

[51] M. Honma, T. Otsuka, T. Mizusaki, and M. Hjorth-Jensen, Phys. Rev. C **80**, 064323 (2009).

[52] J. P. Schiffer, S. J. Freeman, J. A. Clark, C. Deibel, C. R. Fitzpatrick, S. Gros, A. Heinz, D. Hirata, C. L. Jiang, B. P. Kay, A. Parikh, P. D. Parker, K. E. Rehm, A. C. C. Villari, V. Werner, and C. Wrede, Phys. Rev. Lett. **100**, 112501 (2008).

[53] S. V. Szwec, D. K. Sharp, B. P. Kay, S. J. Freeman, J. P. Schiffer, P. Adsley, C. Binnersley, N. de Séréville, T. Faestermann, R. F. Garcia Ruiz, F. Hammache, R. Hertenberger, A. Meyer, C. Portail, I. Stefan, A. Vernon, S. Wilkins, and H.-F. Wirth, Phys. Rev. C **104**, 054308 (2021).

[54] B. P. Kay, T. L. Tang, I. A. Tolstukhin, G. B. Roderick, A. J. Mitchell, Y. Ayyad, S. A. Bennett, J. Chen, K. A. Chipps, H. L. Crawford, S. J. Freeman, K. Garrett, M. D. Gott, M. R. Hall, C. R. Hoffman, H. Jayatissa, A. O. Macchiavelli, P. T. MacGregor, D. K. Sharp, and G. L. Wilson, Phys. Rev. Lett. **129**, 152501 (2022).

[55] S. M. Lenzi, M. A. Bentley, R. Lau, and C. A. Diget, Phys. Rev. C **98**, 054322 (2018).

[56] Data are available at: https://doi.org/10.23729/48d8d431-e698-4fb0-8cc0-01735a3fb11b.